# AI-Assisted Spatio-Temporal Analysis of Forest Cover and Carbon Dynamics in Northeast India: A Remote Sensing and GIS Approach

Arman Khan*

Department of Computer Science & Engineering,
University of Science & Technology Meghalaya, India

**Abstract.** Northeast India is a globally recognised biodiversity hotspot facing severe ecological threats from rapid land-use and land-cover (LULC) changes. This paper presents an original spatio-temporal analysis of forest cover degradation and vegetation health decline at Nameri National Park, Assam, as a primary case study, supported by a regional synthesis of recent AI-assisted remote sensing literature spanning Assam, Arunachal Pradesh, Manipur, and Mizoram. Multi-temporal satellite imagery was accessed freely via Microsoft Planetary Computer and processed in Google Colaboratory using Python. Landsat-8 imagery (2015) and Sentinel-2 imagery (2021, 2026) were classified using K-Means unsupervised machine learning, and three vegetation indices — NDVI, SAVI, and MSAVI — were computed over valid, cloud-free pixels. Results reveal a significant decline in total forest cover from 80.3% (2015) to 69.2% (2026), with dense forest falling sharply from 63.5% to 37.2%. Bare soil and built-up area nearly tripled from 4.3% to 13.7%. Mean NDVI declined from 0.691 to 0.426 on the directly comparable Sentinel-2 platform (2021–2026), and NDVI pixel distribution histograms confirm a landscape-scale shift from a high-NDVI, forest-dominated state toward a fragmented, mixed-cover landscape. These findings provide original quantitative evidence of accelerating forest degradation at Nameri and support the development of open-data geospatial AI workflows as scalable, cost-free tools for ecological monitoring and nature-based climate resilience planning across Northeast India.

**Keywords:** Artificial Intelligence · Carbon Dynamics · Change Detection · GIS · Google Colaboratory · K-Means Classification · Land Use and Land Cover · Microsoft Planetary Computer · Nameri National Park · NDVI · Northeast India · Remote Sensing · Sentinel-2 · Vegetation Indices

## 1 Introduction

Northeast India, nestled within the Eastern Himalaya and Indo-Burma biodiversity hotspots, is an epicentre of ecological wealth and indigenous knowledge [2].

* Under the guidance of Prof. Jainul Abudin, Department of Computer Science & Engineering, University of Science & Technology Meghalaya.

*Proceedings of the First NortheastGenAI Workshop 2026, May 29, 2026* © *2026 Northeast Langchive*

However, the region is highly vulnerable to climate change, land degradation, and resource-use conflicts. The primary drivers of deforestation and forest degradation include agricultural and settlement encroachment, illegal resource extraction, infrastructure development, and shifting cultivation [14].

Monitoring these vast and often inaccessible terrains using traditional ground surveys is a labour-intensive and expensive process. The integration of remote sensing and Geographic Information Systems (GIS) has emerged as a crucial methodology to overcome these limitations. Furthermore, integrating artificial intelligence (AI) and machine learning (ML) algorithms into spatial analyses provides a robust, scalable, and cost-effective approach to automating LULC classification, monitoring biodiversity, and predicting carbon stock dynamics [12].

This paper makes two complementary contributions. First, it presents an original satellite-based analysis of forest cover change and vegetation health at Nameri National Park, Assam, across three time points (2015, 2021, 2026), conducted using entirely free and openly accessible tools and data. Second, it contextualises these original findings within a regional synthesis of recent AI-assisted remote sensing literature for Northeast India. Nameri National Park — a protected area under increasing anthropogenic pressure at the Assam–Arunachal Pradesh border — serves as the primary focus, providing locally specific, multi-date, multi-sensor evidence of landscape-scale forest degradation.

## 2 Study Area: Nameri National Park

Nameri National Park is located in Sonitpur District, Assam, along the foothills of Arunachal Pradesh (approximately 26.75°N–27.05°N, 92.55°E–93.05°E). Established as a national park in 1998, Nameri covers approximately 200 $km^2$ of tropical semi-evergreen and moist deciduous forest, and forms part of a larger elephant and tiger reserve. The park is bisected by the Jia Bhoreli (Kameng) River, a major Brahmaputra tributary whose braided channels and associated sandbars are clearly visible in all satellite imagery acquired for this study.

The landscape is ecologically significant as a corridor between the Nameri Tiger Reserve (Assam) and the Pakke Tiger Reserve (Arunachal Pradesh). It is documented to face increasing threats from agricultural encroachment along its southern and western boundaries, unregulated expansion of eco-tourism infrastructure, and riverine erosion driven by Brahmaputra floodplain dynamics. A GIS-based study of land use dynamics in Nameri from 1988 to 2025 documented a 7.86% decline in open forest cover and a 3.55% expansion of built-up areas [3], providing the literature baseline against which the present original analysis is compared.

## 3 Data Sources and Computational Tools

### 3.1 Satellite Data: Microsoft Planetary Computer

All satellite imagery used in this study was accessed at no cost through the Microsoft Planetary Computer (MPC), a cloud-based geospatial data platform de-

veloped by Microsoft (planetarycomputer.microsoft.com). The Planetary Computer provides a publicly accessible SpatioTemporal Asset Catalog (STAC) API hosting petabytes of Analysis Ready Data (ARD), including the USGS Landsat Collection 2 Level-2 and ESA Sentinel-2 Level-2A archives. Surface reflectance products were retrieved directly from Microsoft Azure cloud storage, requiring no local data download. The STAC API was queried to identify the least-cloudy scene within each dry-season acquisition window, with cloud cover metadata used as the primary scene selection criterion.

**Table 1.** Satellite Data Sources Retrieved from Microsoft Planetary Computer.

| Year | Sensor | Collection | Res. | Date | Cloud | MPC Collection ID |
|---|---|---|---|---|---|---|
| 2015 | Landsat-8 | USGS C2 L2 | 30 m | 2015-11-21 | <10% | landsat-c2-l2 |
| 2021 | Sentinel-2 | ESA L2A | 10 m | 2021-12-19 | <10% | sentinel-2-l2a |
| 2026* | Sentinel-2 | ESA L2A | 10 m | 2025-12-18 | <10% | sentinel-2-l2a |

*Most recent available scene within the Oct 2025–Mar 2026 dry-season window. Valid spatial coverage: 2015 = 239.1 $km^2$ (265,665 pixels at 30 m); 2021 = 238.6 $km^2$ (2,386,008 pixels at 10 m); 2026 = 238.6 $km^2$ (2,386,066 pixels at 10 m). High pixel-count consistency between 2021 and 2026 confirms equivalent spatial coverage for the intra-sensor comparison.

Landsat-8 was selected for the 2015 time point because Sentinel-2A, launched in April 2015, had not yet achieved reliable operational coverage over Northeast India. To maintain consistency within each sensor for the primary trend comparison, all three scenes use the same standard surface reflectance scale factors (Landsat C2 L2: multiply by 0.0000275 and subtract 0.2; Sentinel-2 L2A: divide by 10,000). Inter-sensor differences in band centre wavelengths mean that absolute NDVI values from Landsat-8 and Sentinel-2 are not directly equivalent; accordingly, the 2021–2026 Sentinel-2 pair is treated as the primary intra-sensor comparison throughout the analysis.

### 3.2 Computational Environment: Google Colaboratory

All data processing, classification, and visualisation were performed in Google Colaboratory (Google Colab) [6], a free, browser-based Jupyter notebook environment provided by Google (colab.research.google.com). Colab requires no local installation and provides cloud-based computing resources (CPU runtime), making it accessible without specialist hardware. The complete analysis pipeline — from STAC API querying to figure generation — was executed in a single Colab notebook. This approach demonstrates the full replicability of the workflow using only free, open-access tools.

### 3.3 Python Libraries and Analysis Stack

The following Python libraries were used for the analysis:

**Table 2.** Python libraries used in the analysis.

| Library | Version | Role in This Study |
|---|---|---|
| pystac-client | 0.8.x | Query the Planetary Computer STAC API to search and retrieve satellite scene metadata |
| planetary-computer | 1.0.x | Authenticate and sign asset URLs for direct data access from Microsoft Azure storage |
| odc-stac | 0.3.x | Load multi-band satellite rasters from STAC items into xarray DataArrays, in-cloud without downloading |
| NumPy | 2.2.x | Array operations, vegetation index computation, no-data masking, and statistical summaries |
| scikit-learn | 1.5.x | K-Means unsupervised classification of the multi-band feature stack |
| Matplotlib | 3.9.x | Generation of all figures: NDVI maps, false color composites, classification maps, charts, histograms |
| rioxarray | 0.18.x+ | Geospatial raster handling and coordinate reference system support |

## 4 Methodology

### 4.1 Data Retrieval and Pre-processing

The Planetary Computer STAC API was queried for each time period using a bounding box encompassing Nameri National Park and its immediate surroundings. Scenes were filtered by cloud cover, and the least-cloudy scene within each dry-season window was selected. Surface reflectance scale factors were applied to convert raw digital numbers to physically meaningful reflectance values (range 0–1). A no-data mask was applied by identifying pixels where all spectral bands simultaneously equalled zero — the fill value for scene-edge areas in both Landsat and Sentinel-2 products. All subsequent calculations were performed exclusively on valid, non-masked pixels.

### 4.2 Vegetation Index Computation

Three spectral vegetation indices were calculated for each time point. The Normalised Difference Vegetation Index (NDVI) quantifies general vegetation greenness using near-infrared (NIR) and red bands: $\mathrm{NDVI} = (\mathrm{NIR} - \mathrm{Red})/(\mathrm{NIR} + \mathrm{Red})$. The Soil Adjusted Vegetation Index (SAVI) introduces a soil brightness correction factor $L = 0.5$: $\mathrm{SAVI} = [(\mathrm{NIR} - \mathrm{Red})/(\mathrm{NIR} + \mathrm{Red} + L)] \times (1 + L)$. The Modified SAVI (MSAVI) removes the need for a fixed $L$ parameter: $\mathrm{MSAVI} = [2 \cdot \mathrm{NIR} + 1 - \sqrt{(2 \cdot \mathrm{NIR} + 1)^2 - 8 \cdot (\mathrm{NIR} - \mathrm{Red})}]/2$. SAVI and MSAVI are particularly valuable for Nameri's floodplain and transitional zones where soil exposure is significant. NDVI values above 0.3 are used as the vegetation presence threshold throughout this study [4].

### 4.3 Land Cover Classification

Land cover classification was performed using K-Means unsupervised clustering ($k = 5$) applied to a four-band feature stack of NDVI, NIR, SWIR, and Red reflectance values. Only valid (non-masked) pixels were included in the clustering. Five clusters were ranked by their mean NDVI value and mapped to five land cover classes in ascending order: (1) Water / Wetland, (2) Bare Soil / Built-up, (3) Agriculture / Grassland, (4) Open Forest / Scrub, and (5) Dense Forest. Area statistics were computed as percentages of total valid pixels, and areal extents were calculated using the respective pixel size of each sensor (30 m $\times$ 30 m for Landsat-8; 10 m $\times$ 10 m for Sentinel-2).

### 4.4 Regional Synthesis Methodology

The regional synthesis component draws on peer-reviewed and grey literature from 2022–2026 covering AI-assisted remote sensing studies across Assam, Arunachal Pradesh, Manipur, and Mizoram. Studies were selected based on use of satellite imagery, vegetation indices, and/or machine learning classification methods in Northeast Indian contexts, consistent with the methodological approach of the original Nameri case study.

### 4.5 Classification Accuracy Assessment

The K-Means land cover classification was validated using a spectral rule-based reference approach applied to the 2021 Sentinel-2 scene — the highest-quality acquisition in this study. Reference land cover labels were assigned to each valid pixel using published NDVI threshold criteria for tropical land cover types [4,12]: NDVI $< 0.05$ = Water/Wetland; 0.05–0.20 = Bare Soil/Built-up; 0.20–0.40 = Agriculture/Grassland; 0.40–0.60 = Open Forest/Scrub; $\geq 0.60$ = Dense Forest. A stratified random sample of 2,000 pixels per class (10,000 pixels total) was drawn and the K-Means predictions compared against these reference labels. Classification performance was quantified using Overall Accuracy (OA) and Cohen's Kappa coefficient ($\kappa$), with Kappa interpreted using the Landis & Koch (1977) scale. Producer's Accuracy (omission error) and User's Accuracy (commission error) were computed for each class. This approach provides an internal spectral consistency check appropriate for a study area without contemporaneous field survey data.

## 5 Original Results: Nameri National Park (2015–2026)

### 5.1 NDVI Maps and Vegetation Health

Multi-temporal NDVI maps derived from Landsat-8 (2015) and Sentinel-2 (2021, 2026) imagery reveal a clear and progressive deterioration in vegetation health over the eleven-year study period (Figure 1). In 2015, the study area exhibited predominantly high NDVI values (mean = 0.7312; SAVI = 0.4102; MSAVI =

0.3973) across a valid area of 239.1 km$^2$, with a dense, dark-green canopy dominating the northern forested zone and the park's core area. The 2021 Sentinel-2 map (mean NDVI = 0.6910; range −0.520–0.938; SAVI = 0.3949; MSAVI = 0.3838; valid area = 238.6 km$^2$) shows the forest interior retaining high canopy density, though the large exposed sandbar and active braided channels of the Jia Bhoreli River are clearly identifiable as low-NDVI features consistent with post-monsoon sedimentation patterns. The 2026 Sentinel-2 imagery (mean NDVI = 0.4255; range −0.171–0.726; SAVI = 0.3265; MSAVI = 0.3140; valid area = 238.6 km$^2$) shows a markedly lighter green signature across the landscape, indicating reduced canopy density or widespread vegetation stress.

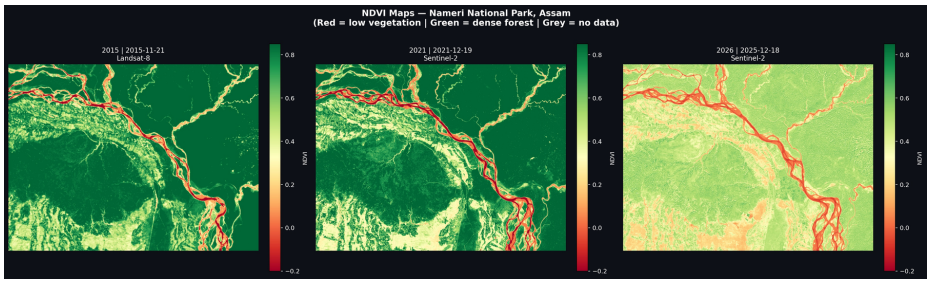


**Fig. 1.** NDVI Maps of Nameri National Park and surrounding landscape for 2015 (Landsat-8, 30 m), 2021 (Sentinel-2, 10 m), and 2026 (Sentinel-2, 10 m). Red = low vegetation; green = dense forest. The progressive shift from deep green (2015) to lighter green (2026) is visible across the landscape.

### 5.2 False Color Composites

False color composites (NIR-Red-Green) confirm the NDVI trend through a qualitative lens (Figure 2). In this band combination, bright red tones indicate strong NIR reflectance from healthy chlorophyll-bearing vegetation. The 2015 composite shows an intensely red landscape with only the river channel appearing as a dark signature. The 2021 composite retains strong red tones in the northern forest zone, with the Jia Bhoreli's braided channels and sandbars visible as grey-tan features. The 2026 composite shows a noticeably paler, less saturated red signature across the floodplain, southern agricultural zones, and peripheral forest areas — visually confirming the quantitative NDVI decline.

### 5.3 Land Cover Classification

K-Means classification maps (Figure 3) and the corresponding area statistics (Table 3, Figure 4) reveal a significant structural shift in the landscape over the study period.

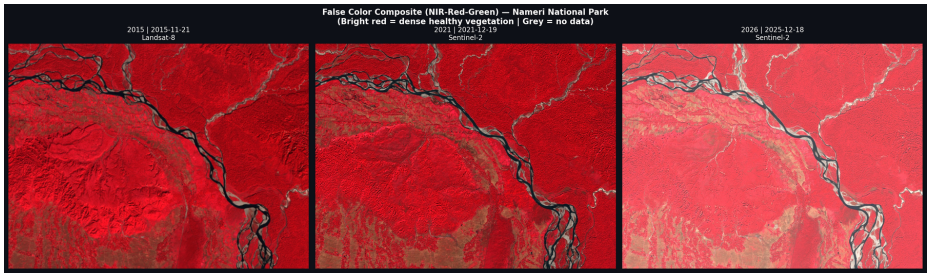


**Fig. 2.** False Color Composite (NIR-Red-Green) for 2015, 2021, and 2026. Bright red = dense healthy vegetation; tan/grey = bare soil or river sandbars; black = open water. The paler red in 2026 across peripheral and floodplain zones is consistent with reduced canopy cover and increasing bare soil exposure.

In 2015, dense forest accounted for 63.5% of valid pixels, open forest/scrub contributed 17.0%, giving a combined forest cover of 80.3%. Agriculture and grassland occupied 13.7% predominantly along the southern floodplain boundary, with minimal bare soil/built-up area (4.3%).

By 2021, the distribution remained broadly stable: dense forest 61.4%, open forest 17.6%, total forest cover 79.0%. This is consistent with Borah (2025), who found limited structural forest loss within the park boundary up to that period. The marginal increases in agriculture (14.8%) and bare soil (4.4%) suggest early-stage peripheral pressure.

The 2026 classification reveals a dramatic structural shift. Dense forest declined sharply to 37.2% — a 26.3 percentage-point reduction from 2015 — while open forest/scrub expanded to 32.0%, suggesting large-scale canopy thinning and transition to secondary or degraded growth. Bare soil and built-up area nearly tripled to 13.7%, consistent with accelerating anthropogenic land conversion in peripheral zones.

**Table 3.** Land Cover Statistics for Nameri National Park Landscape (% of Valid Pixels).

| **Land Cover Class** | **2015 (%)** | **2015 (ha)** | **2021 (%)** | **2021 (ha)** | **2026 (%)** | **2026 (ha)** |
|---|---|---|---|---|---|---|
| Dense Forest | 63.5 | 15,187 | 61.4 | 14,640 | 37.2 | 8,867 |
| Open Forest / Scrub | 16.8 | 4,007 | 17.6 | 4,200 | 32.0 | 7,629 |
| Agriculture / Grassland | 13.7 | 3,281 | 14.8 | 3,526 | 13.8 | 3,300 |
| Bare Soil / Built-up | 4.3 | 1,026 | 4.4 | 1,047 | 13.7 | 3,267 |
| Water / Wetland | 1.7 | 410 | 1.9 | 447 | 3.3 | 798 |
| **Total Forest Cover** | **80.3** | **19,194** | **79.0** | **18,840** | **69.2** | **16,496** |

Note: Hectare estimates based on 30m pixel (Landsat-8) and 10m pixel (Sentinel-2) areas respectively.

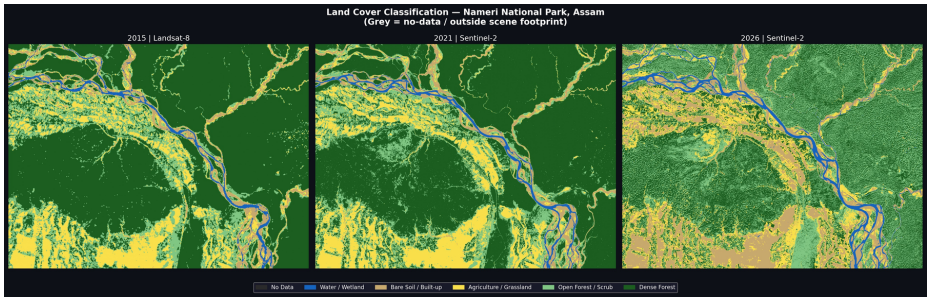


**Fig. 3.** Land Cover Classification Maps for Nameri National Park landscape for 2015 (Landsat-8), 2021 (Sentinel-2), and 2026 (Sentinel-2), produced by K-Means unsupervised classification. Dark green = Dense Forest; light green = Open Forest/Scrub; yellow = Agriculture/Grassland; tan = Bare Soil/Built-up; blue = Water/Wetland; grey = no-data.

### 5.4 Forest Cover Change Trend Analysis

The forest cover trend chart (Figure 4) summarises the key trajectories. Total forest cover declined by 11.2 percentage points over eleven years. The decline was gradual between 2015 and 2021 (−1.3 pp) but accelerated sharply between 2021 and 2026 (−9.9 pp), suggesting that deforestation pressures intensified significantly in the most recent five-year period. The dense forest component drove the majority of this change, declining from 63.5% to 37.2%. The concurrent rise in open forest/scrub (16.8% to 32.0%) indicates canopy thinning and degradation — where trees remain but the canopy has opened — rather than outright forest clearance. The near-tripling of bare soil and built-up area (4.3% to 13.7%) points to expanding anthropogenic footprint in the landscape's peripheral zones.

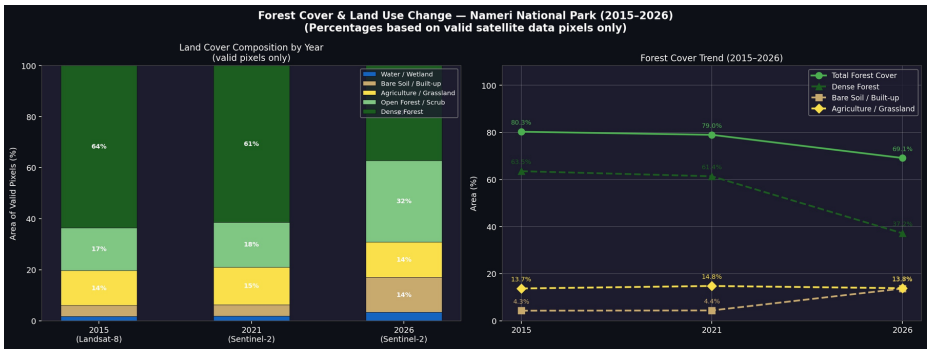


**Fig. 4.** Left: Stacked bar chart showing land cover composition by year (% of valid pixels). Right: Trend lines for total forest cover, dense forest, bare soil/built-up, and agriculture/grassland (2015–2026). All values are based on valid satellite data pixels only. Sensor labels indicate the respective platform for each time point.

### 5.5 Vegetation Index Comparison

All three vegetation indices — NDVI, SAVI, and MSAVI — exhibit the same directional decline (Figure 5). On the directly comparable Sentinel-2 platform, NDVI declined from 0.691 (2021) to 0.425 (2026), a 38.5% relative reduction (absolute change of −0.2655 NDVI units). SAVI declined from 0.395 to 0.327, and MSAVI from 0.384 to 0.314. The convergence of all three indices — including two soil-brightness-corrected indices — strengthens confidence that the observed decline reflects genuine vegetation loss or degradation rather than sensor noise or soil background effects.

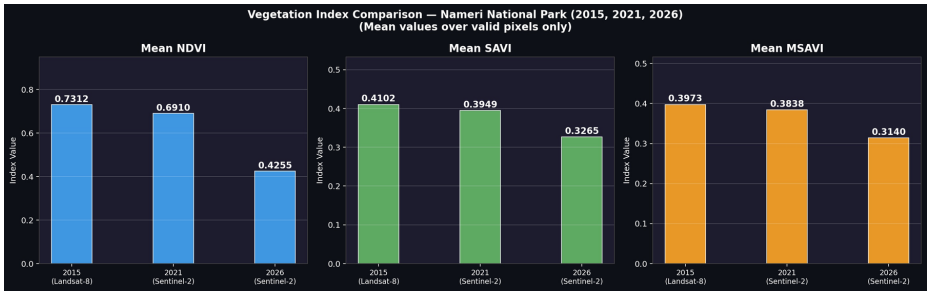


**Fig. 5.** Mean vegetation index values (NDVI, SAVI, MSAVI) for Nameri National Park landscape across 2015 (Landsat-8), 2021 (Sentinel-2), and 2026 (Sentinel-2). All means are computed over valid (non-masked) pixels only. The 2021–2026 Sentinel-2 comparison represents the most directly sensor-consistent trend.

### 5.6 NDVI Pixel Distribution Analysis

The NDVI pixel distribution histograms (Figure 6) provide the most diagnostic visualisation of landscape-scale change. In 2015, the distribution is tightly concentrated in the high-NDVI range (0.6–0.9), with the vast majority of pixels well above the 0.3 vegetation threshold — a signature of a predominantly intact, closed-canopy forest landscape. Almost no pixels fall below 0.3, indicating negligible bare soil or heavily degraded cover.

By 2021, the distribution broadens slightly while retaining a dominant high-NDVI peak around 0.85–0.90. A secondary, smaller peak emerges around 0.25–0.35, corresponding to the agriculture and grassland class in the floodplain zone. This bimodal pattern indicates the beginning of landscape bifurcation between forested and non-forested land.

The 2026 distribution represents a fundamentally different landscape. The mean has shifted left to 0.425, and the distribution spreads broadly from negative values (open water/sandbars) through 0.0–0.2 (bare soil, sparse cover) to a peak around 0.45–0.60 (open forest/degraded canopy). The high-NDVI peak characteristic of 2015 and 2021 has collapsed in relative terms, replaced by a

broad, low-to-moderate NDVI signature. The proportion of pixels below the 0.3 vegetation threshold has increased substantially, confirming that a significant fraction of the landscape no longer supports healthy vegetation cover.

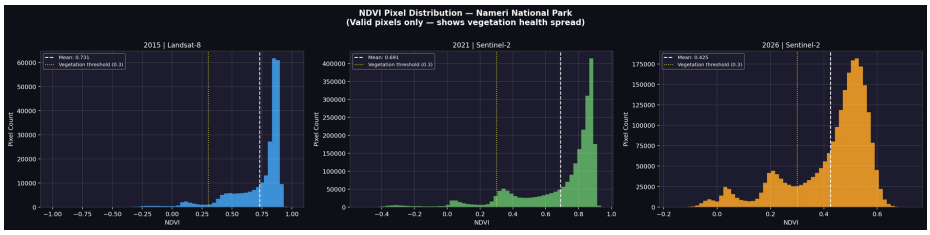


**Fig. 6.** NDVI pixel distribution histograms for Nameri National Park landscape for 2015, 2021, and 2026. Each histogram shows only valid (non-masked) pixels. The white dashed line marks the mean NDVI; the yellow dotted line marks the 0.3 vegetation presence threshold. The dramatic leftward shift and broadening of the 2026 distribution relative to 2015–2021 confirms landscape-scale vegetation degradation.

### 5.7 Classification Accuracy Assessment

The spectral rule-based accuracy assessment of the 2021 Sentinel-2 K-Means classification yielded an Overall Accuracy (OA) of 69.1% and a Cohen's Kappa coefficient of $\kappa = 0.614$, indicating Substantial agreement between the K-Means classification and the NDVI-threshold reference labels [9]. The confusion matrix and per-class accuracy chart are presented in Figure 7.

At the class level, Bare Soil / Built-up achieved perfect Producer's Accuracy (100.0%), confirming highly reliable detection of exposed and built-up surfaces. Agriculture / Grassland also performed strongly (Producer's Accuracy 86.8%), reflecting clear spectral separability of cropland and grassland NDVI signatures. Water / Wetland achieved 75.2% Producer's Accuracy with 100% User's Accuracy, indicating all classified water pixels are correct though some are missed.

The greatest classification uncertainty occurred at the Open Forest / Scrub and Dense Forest boundary, with Open Forest achieving only 40.4% Producer's Accuracy and 24.9% User's Accuracy. This reflects the well-documented spectral overlap between transitional and mature canopy at intermediate NDVI values, which is a known limitation of unsupervised K-Means classification without field-validated training samples [12]. Dense Forest achieved a high User's Accuracy of 100% — indicating that all pixels labelled Dense Forest by K-Means are spectrally consistent with dense canopy — but a Producer's Accuracy of 57.1%, suggesting some dense forest pixels were assigned to the Open Forest class. The reported Dense Forest area values (Table 3) may therefore represent a conservative underestimate. The overall land cover change trend — and in particular the consistent decline in combined forest cover and rise in bare soil — remains robust to this inter-class confusion.

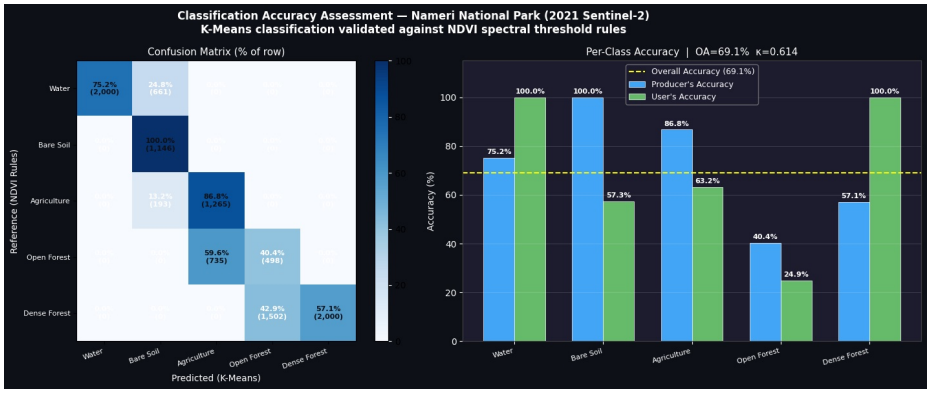


**Fig. 7.** Classification accuracy assessment for the 2021 Sentinel-2 K-Means classification validated against NDVI spectral threshold reference labels (10,000 stratified sample pixels). Left: Confusion matrix showing row-normalised percentage agreement. Right: Per-class Producer's and User's accuracy. Overall Accuracy = 69.1%; Cohen's Kappa = 0.614 (Substantial agreement).

## 6 Regional Spatio-Temporal Analysis: Northeast India

The Nameri findings are consistent with — and extend — a broader pattern of AI-assisted remote sensing studies documenting forest degradation across Northeast India. In Arunachal Pradesh's Lower Dibang Valley, machine learning classification of Landsat data from 2009 to 2021 indicated an 8% decrease in forest area and a 6% decrease in rangeland and scrubland, with these landscape changes independently impacting climatic variables such as temperature, precipitation, and specific humidity [12]. In Assam, broader spatial analysis reveals that 10,076.43 square kilometres of forest experienced degradation between 2000 and 2022 [14]. Dense vegetation increases were recorded in localised zones of Assam's Lakhimpur district, attributed to targeted tree plantations by forest committees and canopy maintenance in tea estates [4] — a finding that underscores the potential of community-managed regreening as a partial counterforce to broader degradation trends.

Multi-spectral analysis in Manipur from 2018 to 2023 highlighted rapid urban sprawl, with bare soil expanding from approximately 343 $km^2$ to 523 $km^2$ — a trajectory strikingly similar to the near-tripling of bare soil observed at Nameri over a comparable period [11]. In Mizoram, a comparative analysis of Aizawl from 2006 to 2012 found that a decline in shifting cultivation — likely driven by government-introduced permanent cultivation policies — correlated with a regional increase in forest cover, demonstrating that policy interventions can produce measurable satellite-detectable recovery [8].

# 7 Carbon Stock Dynamics and Climate Resilience

The integration of spatial intelligence extends beyond LULC mapping to the critical assessment of regional carbon pools. Forests act as terrestrial carbon sinks, sequestering carbon in aboveground biomass, belowground roots, and soil. Satellite-derived vegetation indices are utilised to estimate tree volume and aboveground biomass. Studies synthesising biomass data across Northeast India report an average total biomass carbon estimate of 136.86 megagrams per hectare for aboveground biomass, with aboveground biomass contributing the vast majority of the total carbon pool [5]. Standardised IPCC benchmarks estimate that carbon constitutes approximately 47% of dry living biomass in these tropical ecosystems, and below-ground biomass constitutes a further 26% of aboveground biomass.

## 7.1 Estimated Carbon Stock Change at Nameri (2015–2026)

Using the classification-derived forest area estimates (Table 3) combined with the regional biomass reference values from Dasgupta & Das (2025) and IPCC below-ground biomass ratios, this study computes an original estimate of carbon stock change at Nameri National Park. Dense forest total biomass (aboveground + below-ground) is estimated at 172.44 Mg/ha; open forest at 107.10 Mg/ha. Applying a carbon fraction of 0.47, the estimated total carbon stock declined from 1,432,539 Mg C in 2015 to 1,102,664 Mg C in 2026 — a net loss of 329,876 Mg C over eleven years (Table 4).

**Table 4.** Estimated Carbon Stock by Forest Type — Nameri National Park (2015–2026).

| Year / Sensor | Dense Forest (Mg C) | Open Forest (Mg C) | Total (Mg C) | Change from 2015 (Mg C) |
|---|---|---|---|---|
| 2015 (Landsat-8) | 1,230,859 | 201,680 | 1,432,539 | — |
| 2021 (Sentinel-2) | 1,186,534 | 211,425 | 1,397,959 | −34,580 |
| 2026 (Sentinel-2) | 718,633 | 384,031 | 1,102,664 | −329,876 |

Biomass references: Dasgupta & Das (2025); IPCC below-ground ratio = 0.26; carbon fraction = 0.47. Hectare values from Table 3.

Expressed as $CO_2$ equivalent ($C \times 44/12$), the net carbon loss over eleven years represents approximately 1,209,544 Mg $CO_2$e (approximately 1.21 million tonnes $CO_2$e). The annualised rate of carbon loss averages 29,989 Mg C per year (≈109,959 Mg $CO_2$e per year). To contextualise this figure: 109,959 tonnes of $CO_2$e per year is equivalent to the annual emissions of approximately 23,900 passenger vehicles, underscoring the climate significance of forest loss even at a single protected-area scale.

These estimates carry inherent uncertainty arising from three sources: (i) the K-Means classification accuracy of 69.1%, particularly the under-estimation of dense forest area discussed in Section 5.7; (ii) the use of regional average rather than site-specific biomass values; and (iii) the absence of below-ground soil

carbon, which would increase the true carbon loss figure. The estimates should therefore be interpreted as conservative lower-bound indicators of carbon stock change, suitable for policy-level awareness and directing future field-validated carbon inventories.

### 7.2 Regional Carbon Context and Conservation Implications

Crucially, the highest biomass and carbon sequestration rates across Northeast India are recorded in traditionally protected areas, such as the sacred groves of Manipur and Meghalaya, underscoring the effectiveness of indigenous conservation practices in maintaining old-growth trees and ecosystem stability [5]. The partial recovery of open forest area at Nameri between 2015 and 2026 — from 4,007 ha to 7,629 ha — provides a partial carbon offset of approximately 182,351 Mg C, limiting the gross dense forest carbon loss of 512,226 Mg C to a net loss of 329,876 Mg C. This underscores the importance of protecting transitional and secondary forest as a carbon buffer even where primary forest is being lost. Remote sensing is also actively used to identify aquifer recharge zones for springshed management and to monitor wetland restoration for flood resilience [2] — applications where the free-tool workflow demonstrated in this study could be directly replicated across the region.

## 8 Conclusion

This study demonstrates that free and openly accessible tools — Microsoft Planetary Computer for satellite data and Google Colaboratory for cloud computing — can support fully reproducible, original scientific analysis of forest cover change at a nationally significant protected area. The original analysis of Nameri National Park reveals an alarming trajectory: total forest cover declined by 11.2 percentage points between 2015 and 2026, dense forest fell from 63.5% to 37.2%, and bare soil and built-up area nearly tripled. The decline accelerated markedly between 2021 and 2026, and is confirmed independently by NDVI ($-0.2655$ on Sentinel-2), SAVI, MSAVI, and pixel distribution histograms. Classification accuracy was assessed at 69.1% Overall Accuracy ($\kappa = 0.614$, Substantial agreement). Carbon stock estimates derived from the classification indicate a net loss of approximately 329,876 Mg C (1.21 million tonnes $CO_2e$) over eleven years — equivalent to roughly 109,959 tonnes $CO_2e$ per year — providing the first satellite-derived carbon change estimate for this landscape. These findings both extend the earlier Borah (2025) study and provide a more recent, higher-resolution, and quantitatively detailed perspective on degradation dynamics at Nameri.

At the regional scale, the synthesis of literature across Assam, Arunachal Pradesh, Manipur, and Mizoram confirms that the Nameri trajectory is part of a wider pattern of AI-detectable forest degradation across Northeast India, driven by agriculture, urbanisation, infrastructure, and shifting cultivation. The

exception of Mizoram, where policy-driven agricultural shifts correlated with forest recovery, points to the power of targeted governance interventions.

To achieve sustainable development goals for the region, policymakers must integrate geospatial AI workflows — of the kind demonstrated here — into ongoing ecological monitoring systems, using them to identify degradation hotspots, design nature-based solutions, and track conservation outcomes in near-real-time. Future research should integrate field-validated biomass sampling with the satellite-derived indices produced here to validate and refine carbon stock estimates, and should leverage Sentinel-2's five-day revisit cycle for high-frequency, intra-annual disturbance monitoring.

**AI Transparency Statement** In accordance with the NortheastGenAI 2026 open experiment guidelines, this paper was developed with the assistance of Claude [1], an AI language model. Claude was used to support manuscript structuring and drafting, and to generate the Python analysis code used in Google Colaboratory for satellite data retrieval, vegetation index computation, K-Means classification, and figure generation. The satellite imagery retrieval, execution of all code, verification of analytical outputs, and scientific interpretation were performed by the human author. The research direction, study area selection, time period choices, and final editorial oversight were determined entirely by the human author and supervising professor.

Google NotebookLM [7] was used to organise and cross-reference literature sources during the regional synthesis phase. Perplexity AI [13] was used for exploratory background research to identify relevant studies.

## References

1. Anthropic: Claude (claude.ai). Anthropic, PBC (2026). `https://claude.ai`
2. Behera, M.D.: Towards achieving sustainable development goals in Northeast India: Scaling nature-based solutions with geospatial technology. G.B. Pant National Institute of Himalayan Environment (2025)
3. Borah, A.: Tourism, livelihoods and landscape change: A GIS-based study of land use dynamics in Nameri National Park, Assam. In: Proceedings of the International Conference on Smart Systems and Social Management. Atlantis Press (2025)
4. Borgohain, P., Bora, J.: Change detection analysis in vegetation cover using remote sensing and GIS for Nowboicha Revenue Circle of Lakhimpur District, Assam. International Journal of Innovative Research in Technology **11**(12) (2025)
5. Dasgupta, P., Das, D.J.: Forest types, biomass and carbon dynamics in the Northeastern states of India: A comprehensive review. Environment and Ecology **43**(2), 510–521 (2025)
6. Google: Google Colaboratory. Google LLC (2024). `https://colab.research.google.com`
7. Google: NotebookLM. Google LLC (2024). `https://notebooklm.google.com`
8. Lalhmachhuana, H., Lalnuntluanga, Lalramdina: Analysis of land use land cover change using remote sensing and geographical information system at Aizawl district, Mizoram, India. Journal of Emerging Technologies and Innovative Research **9**(7) (2022)

9. Landis, J.R., Koch, G.G.: The measurement of observer agreement for categorical data. Biometrics **33**(1), 159–174 (1977)
10. Microsoft: Planetary Computer data catalogue. Microsoft Corporation (2024). https://planetarycomputer.microsoft.com/catalog
11. Nivia, O., Mishra, N., Oinam, B., Gupta, K.K., Kunwar, S.: Vegetation cover mapping and change detection analysis using multi-temporal satellite imagery: A case study of Imphal East & West districts. Environment Conservation Journal **27**(1), 377–395 (2026)
12. Patil, P., Patil, C., Musalvad, S., Sahoo, U.K., Janardhana, S.T., Kumar, S., Lyngdoh, N.: Monitoring land use land cover change and its impact on climatic parameters using remote sensing and GIS: A case study of Lower Dibang Valley, Arunachal Pradesh, India. Geoinformatica Polonica **23**, 59–75 (2024)
13. Perplexity AI: Perplexity. Perplexity AI, Inc. (2025). https://www.perplexity.ai
14. TERI: Drivers of degradation and decrease in forest cover of Assam. Assam Project on Forest and Biodiversity Conservation Society (2024)
15. USGS: Landsat Collection 2 Level-2 Science Product Guide. U.S. Geological Survey (2024). https://www.usgs.gov/landsat-missions